Turk J Chem
33 (2009) , 333 – 345.

doi:10.3906/kim-0809-24

A density functional theory study of oxidation of benzene to phenol by N_2O on Fe- and Co-ZSM-5 clusters

Mehmet Ferdi FELLAH[1,2], **Işık ÖNAL**[1,*]
[1] *Department of Chemical Engineering, Middle East Technical University, Ankara, 06531, TURKEY*
[2] *Department of Chemical Engineering, Yüzüncü Yıl University, Van, 65080, TURKEY*
e-mail: ional@metu.edu.tr

Received 17.09.2008

Density functional theory (DFT) calculations were carried out in the study of oxidation of benzene to phenol by N_2O on relaxed $[(SiH_3)_4AlO_4M]$ (where M=Fe, Co) cluster models representing Fe- and Co-ZSM-5 surfaces. The catalytic cycle steps are completed for both Fe-ZSM-5 and Co-ZSM-5 clusters. The general trend of the results that were obtained in terms of activation barriers for the Fe-ZSM-5 cluster is in agreement with the experimental and theoretical literature. It was observed that the phenol formation step is the rate-limiting step for both clusters and Co-ZSM-5 surface has a lower activation barrier than the Fe-ZSM-5 surface (i.e. 35.82 kcal/mol vs. 45.59 kcal/mol, respectively).

Key Words: DFT, benzene oxidation, phenol, N_2O, Fe-ZSM-5, Co-ZSM-5.

Introduction

The predominant use of phenol as an important chemical raw material is in the production of bisphenol, phenolic resins, caprolactam, aniline, and alkylphenols. In 2001, worldwide phenol has been producted was nearly 6.4 million metric tons.[1] Phenol is produced by the cumene process, which has some definite disadvantages such as poor ecology, an explosive intermediate (cumene hydroperoxide), and a multistep character.[2] The direct oxidation of benzene to phenol is an alternative process to the cumene process. Fe-ZSM-5 zeolite was used as a catalyst for the direct benzene oxidation to phenol[3] with oxygen (O_2) or nitrous oxide (N_2O) as oxidants. Panov and co-workers[3] have reported that with nitrous oxide benzene conversion reaches 27% at 350 °C,

*Corresponding author

whereas it is only 0.3% at 500 °C in the presence of oxygen. It is also reported that with N_2O as the oxidant phenol forms with a high selectivity (98%), while with O_2 only complete oxidation occurs. Several studies[3–21] have demonstrated that Fe-ZSM-5 can be used to produce phenol from C_6H_6 and N_2O. Hensen et al.[20,21] have reported that [Fe,Al]MFI shows good performance in selective oxidation of benzene to phenol. It is reported in both the experimental[4,5,13,22–24] and theoretical[25–29] literature that the α-form of the surface oxygen formed by decomposition of N_2O plays an important role in the direct oxidation of benzene on Fe-ZSM-5. It is experimentally[30–38] and theoretically[39–45] reported that Fe and Co-exchanged ZSM-5 are active catalysts for the stoichiometric decomposition of N_2O to form the α-form of the surface oxygen and benzene is selectively oxidized to phenol over the interaction with the α-form of the surface oxygen produced on Fe-ZSM-5 zeolite by N_2O decomposition.[4,5,13,22–24] The following reactions are also proposed for the direct oxidation of benzene by N_2O;[2,23,24]

$$N_2O + (\ )_\alpha \rightarrow (O)_\alpha + N_2 \tag{1}$$

$$(O)_\alpha + C_6H_6 \rightarrow (C_6H_5OH)_\alpha \tag{2}$$

$$(C_6H_5OH)_\alpha \rightarrow C_6H_5OH + (\ )_\alpha \tag{3}$$

The surface oxygen $(O)_\alpha$ formed in reaction 1 on Fe-ZSM-5 by decomposition of N_2O is responsible for the formation of phenol from benzene (reaction 2). The phenol product can be finally desorbed from the surface (reaction 3). Yoshizawa et al.[26] studied the reaction pathways and the energetics for the direct benzene oxidation to phenol on Fe-ZSM-5 zeolite represented as a $[(SiH_3)_2AlO_2(OH)_2(FeO)]$ cluster. They reported that the surface oxygen species is responsible for the catalytic reactivity of the Fe-ZSM-5 zeolite. Ryder et al.[25] have studied benzene oxidation to phenol over Fe-ZSM-5 cluster modeled as $(SiH_3)_4AlO_4(FeO)$ and as $(SiH_3)4AlO_4(FeO_2)$. They reported that both (FeO) and (FeO_2) are active centers of the clusters for the direct oxidation of benzene. The intermediates of the benzene oxidation to phenol by N_2O have been investigated theoretically on Fe-ZSM-5 cluster by Kachurovskaya et al.[29] Neither the experimental nor the theoretical literature contains studies on benzene oxidation to phenol by N_2O on Co-ZSM-5. Recently we have theoretically reported that an α-oxygen formation reaction by N_2O decomposition (reaction 1) occurs on Fe- and Co-ZSM-5 clusters with a high exothermic relative energy through a very small activation barrier[44].

The aim of this study was to investigate the catalytic oxidation of benzene to phenol by nitrous oxide and to identify the mechanistic steps by use of the density functional theory (DFT) calculations. ZSM-5 is modeled as a $[(SiH_3)_4AlO_4M]$ (M=Fe, Co) cluster. DFT calculations with B3LYP formalism using 6-31G** as a basis set are utilized to obtain energy profiles and equilibrium geometries.

Surface models and calculation method

All calculations in this study are based on DFT,[46] which is implemented in the Gaussian 2003 suit of programs.[47] Becke's[48,49] 3-parameter hybrid method involving the Lee, Yang, and Parr[50] correlation functional (B3LYP) formalism using 6-31G** as the basis set was utilized. The ZSM-5 structure shown in Figure 1(a) was constructed by using the Cartesian coordinates reported by Lermer et al.[51] A ZSM-5 cluster including 5 Si and 4 O atoms is cut from inside a channel (see Figure 1(b)) and the ZSM-5 clusters used in this study were modeled as

$[(SiH_3)_4AlO_4M]$ (M=Fe, Co) clusters as shown in Figure 1(c). The dangling bonds of the terminal silicon atoms are terminated with H atoms to obtain a neutral cluster. The reactant and product molecules as well as all of the cluster atoms were kept relaxed. Energy profile, equilibrium geometry (EG), and transition state (TS) calculations were performed for determination of the activation barriers and relative reaction energies.

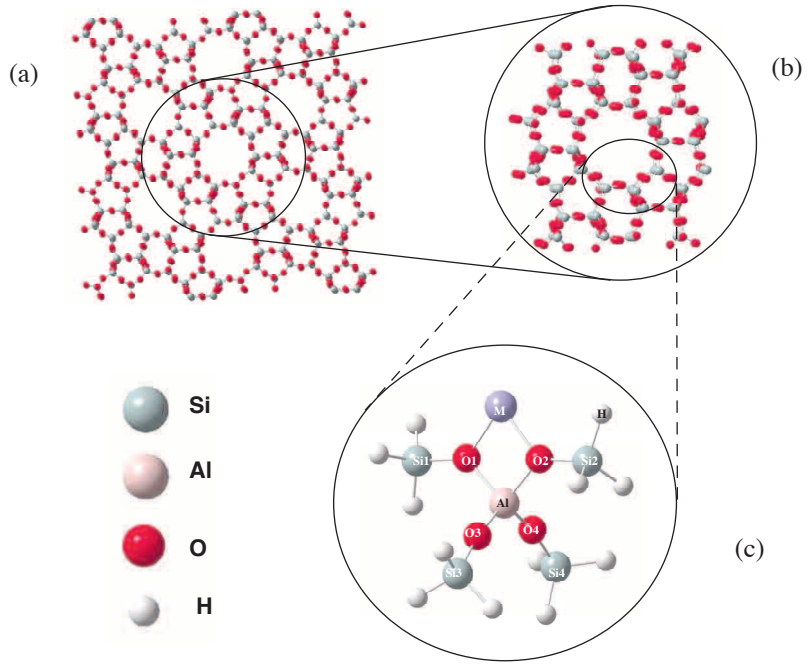

Figure 1. (a) ZSM-5 zeolite, (b) ZSM-5 channel, (c) Optimized geometries M-ZSM-5 cluster (where M=Fe, Co).

The computational strategy employed in this study was as follows. Initially, the correct spin multiplicity of the system consisting of cluster and adsorbing molecules was determined by single point energy (SPE) calculations. SPEs were calculated with different spin multiplicity numbers for each cluster system and the spin multiplicity number that corresponds to the lowest SPE was regarded as the correct spin multiplicity. The cluster and the adsorbing molecules, N_2O and C_6H_6, are then fully optimized geometrically by means of EG calculations.

The adsorbing molecule is first located over the active site of the cluster at a selected distance and a coordinate driving calculation was performed by selecting a reaction coordinate in order to obtain the variation in the relative energy with a decreasing reaction coordinate to get an energy profile as a function of the selected reaction coordinate distance. Single point equilibrium geometry calculations were also performed where necessary by locating the adsorbing molecule in the vicinity of the catalytic cluster. Coordinate driving calculations result in an energy profile. The resulting relative energies for the cluster and reactant molecule complex are plotted against the reaction coordinate. The relative energy was defined with the following formula:

$$\Delta E = E_{\text{System}} - (E_{\text{Cluster}} + E_{\text{Adsorbate}})$$

where E_{System} is the calculated energy of the given geometry containing the cluster and the adsorbing molecule at any distance, $E_{Cluster}$ is the energy of the cluster, and $E_{Adsorbate}$ is that of the adsorbing molecule, e.g. N_2O

or C_6H_6 in this case. After obtaining the energy profile for the reaction step, the geometry with the minimum energy on the energy profile was re-optimized by means of EG calculations to obtain the final geometry for the particular reaction step. In this re-optimization calculation, the reaction coordinate is not fixed. Additionally, the geometry with the highest energy from the energy profile is taken as the input geometry for the transition state geometry calculations. Starting from these geometries, the transition state structures with only one negative eigenvalue in the Hessian matrix are obtained. Transition states have been calculated using the synchronous quasi-Newtonian method of optimization, QST3.[52]

Results

a. Optimization of clusters and reactant molecules

EGs for Co- and Fe-ZSM-5 clusters were obtained taking the total charge as neutral, and the spin multiplicities corresponding to the lowest SPE were determined to be 5 and 6, respectively. The optimized geometries of a ZSM-5 cluster with a single M site (M=Fe, Co) are depicted in Figure 1(c). Si-O distances for M-ZSM-5 clusters range from 1.63 A to 1.68 A. The corresponding distances reported earlier in the experimental literature are between 1.55 A and 1.65 A[51]. Similarly, M-O (M=Fe, Co) distances were calculated as 2.005 A and 2.006 A for Fe-ZSM-5 cluster and 1.975 A and 1.979 A for the Co-ZSM-5 cluster. Average Si-H distance was calculated as 1.485 A for these clusters.

EGs for N_2O and C_6H_6 as reactant molecules were obtained by taking the total charge as zero and with a singlet spin multiplicity. The optimized linear N_2O molecule has a distance of 1.134 A for N-N bond and 1.192 A for N-O bond. The corresponding values were reported to be 1.128 A and 1.185 A in the experimental literature.[53] Linear (N-N-O) N_2O molecule was used for decomposition reaction calculations on all clusters. The calculated C-H bond distance value of 1.397 A and C-C bond distance value of 1.082 A of benzene molecule are very close to the previously reported experimental values of 1.399 A and 1.084 A, respectively[54].

b. Oxidation of benzene on M-ZSM-5 (M=Fe, Co) clusters

The proposed reaction steps, which are given in detail in the References,[2,23,24] for the cycle of benzene oxidation by N_2O on a mononuclear site on M-ZSM-5 are

$$M-\text{cluster} + N_2O \rightarrow O-M-\text{cluster} + N_2$$

(Step 1, N_2O decomposition) (4)

$$O-M-\text{cluster} + C_6H_6 \rightarrow HO-M-\text{cluster} + C_6H_5$$

(Step 2, C-H bond activation of C_6H_6) (5)

$$HO-M-\text{cluster} + C_6H_5 \rightarrow HO-M-C_6H_5-\text{cluster}$$

(Step 3, hydroxy complex formation) (6)

$$H-O-M-C_6H_5-\text{cluster} \rightarrow M-C_6H_5OH-\text{cluster}$$

(Step 4, phenol formation) (7)

$$M - C_6H_5OH - \text{cluster} \rightarrow M - \text{cluster} + C_6H_5OH$$

(Step 5, phenol desorption) (8)

b1. Oxidation of benzene on Fe-ZSM-5 cluster

Decomposition of the N_2O molecule on the Fe-ZSM-5 cluster is the first reaction step (step 1) as reported in our previous study.[44] The second and third steps (C-H bond activation of C_6H_6 and third step hydroxy complex formation, respectively) occur simultaneously on the FeO-ZSM-5 cluster. A reaction coordinate was selected as the distance between the hydrogen atom (H) of the C_6H_6 molecule and oxygen atom (O5) adsorbed on the cluster during the first step. The relative energy profile obtained is depicted in Figure 2. This reaction occurs with an exothermic relative energy difference of -20.80 kcal/mol through an activation barrier (TS) of 20.29 kcal/mol. The calculated imaginary frequency related with the transition state mode is 1674i cm^{-1}. The corresponding O-H distance for the transition state was found as 1.259 A. The next reaction was the formation of phenol on the FeO-ZSM-5 cluster. For this step, a reaction coordinate was selected as the distance between the oxygen atom (O5) and carbon atom (C1) of the adsorbed phenyl ring. The relative energy profile obtained is presented in Figure 3. This reaction has an endothermic relative energy difference of 44.82 kcal/mol through a higher activation barrier (TS) of 45.59 kcal/mol as compared to those for steps 1, 2, and 3. The calculated imaginary frequency related to the transition state mode was 261i cm^{-1}. The corresponding C-O distance for the transition state was 1.713 A.

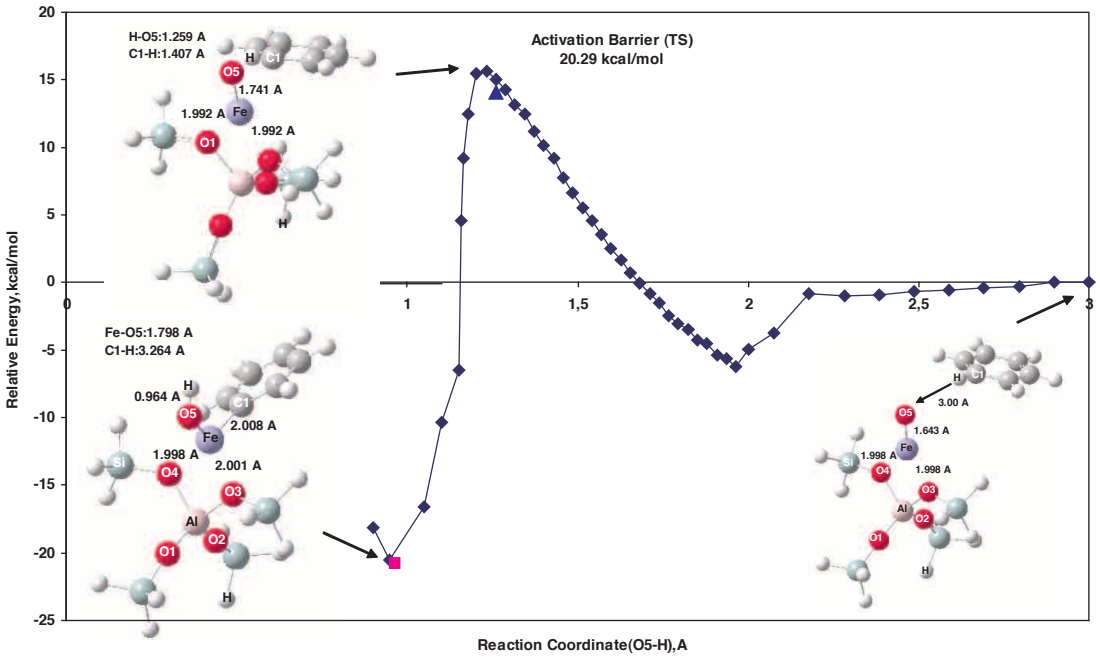

Figure 2. Relative energy profile, transition state, and final equilibrium geometries for C-H bond activation of C_6H_6 and hydroxy complex formation (steps 2 and 3) on FeO-ZSM-5 cluster.

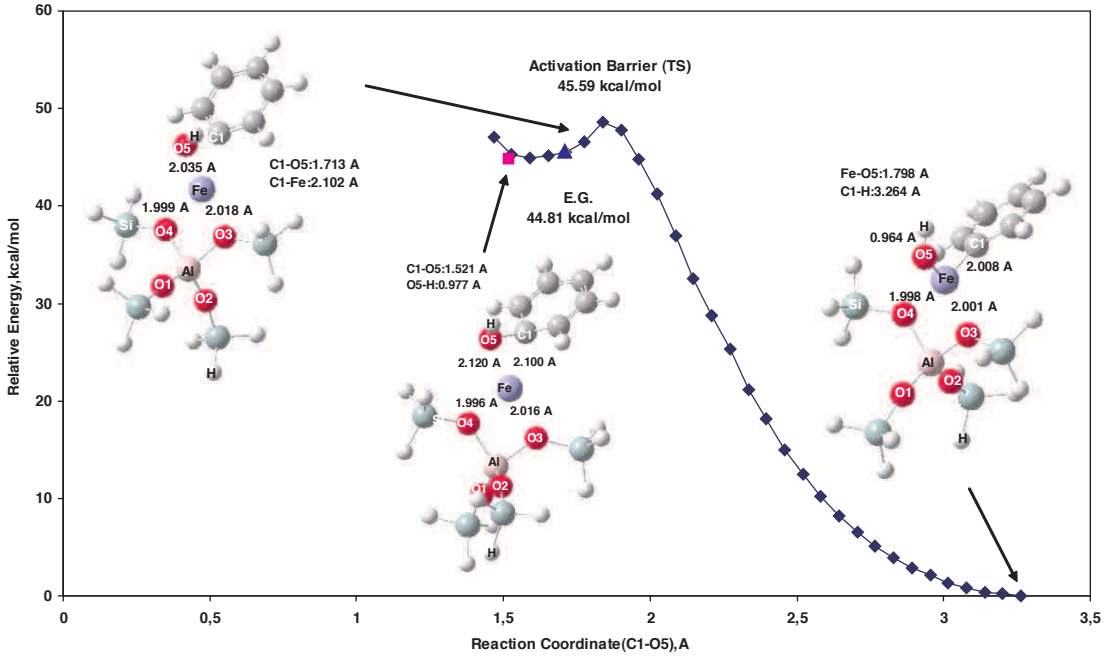

Figure 3. Relative energy profile, transition state, and final equilibrium geometries for phenol formation reaction (step 4) on FeO-ZSM-5 cluster.

Finally, the last reaction step (step 5) is the desorption of phenol that is formed on the cluster. For this step, a reaction coordinate is selected as the distance between the oxygen atom (O5) of the phenol molecule and the Fe atom of the cluster. This reaction has a very small desorption barrier of 5.65 kcal/mol as compared the other steps.

b2. Oxidation of benzene on Co-ZSM-5 cluster

The first reaction (step 1), the decomposition of the N_2O molecule on the Co-ZSM-5 cluster, was already reported similarly in our previous study.[44] For the second step, the C-H bond activation of benzene molecule, a reaction coordinate was selected as the distance between the hydrogen atom (H) of the C_6H_6 molecule and oxygen atom (O5) adsorbed on the cluster during the first step. The relative energy profile obtained is depicted in Figure 4. This reaction occurs with an endothermic relative energy difference of 16.83 kcal/mol through an activation barrier (TS) of 20.58 kcal/mol. The calculated imaginary frequency related to the transition state mode is 1515 cm^{-1}. The corresponding O-H distance for the transition state is 1.141 A.

The third step, hydroxy complex formation, is the reaction between C_6H_5 radical and Co atom of the cluster. For this reaction, a reaction coordinate was selected as the distance between the carbon atom (C1) of the phenyl radical and Co atom of the cluster. This reaction seems to occur on the cluster with an exothermic relative energy difference of -31.57 kcal/mol and its relative energy profile obtained is represented in Figure 5. The next reaction is the formation of phenol on the CoO-ZSM-5 cluster. For this step, a reaction coordinate was selected as the distance between the oxygen atom (O5) and C1 atom of the adsorbed C_6H_5 group. The relative energy profile obtained is given in Figure 6. This reaction has an endothermic relative energy difference

of 35.11 kcal/mol through an activation barrier (TS) of 35.82 kcal/mol as compared to steps 1, 2, and 3. The calculated imaginary frequency related with the transition state mode is 257i cm^{-1}. The corresponding C-O distance for the transition state is 1.718 A.

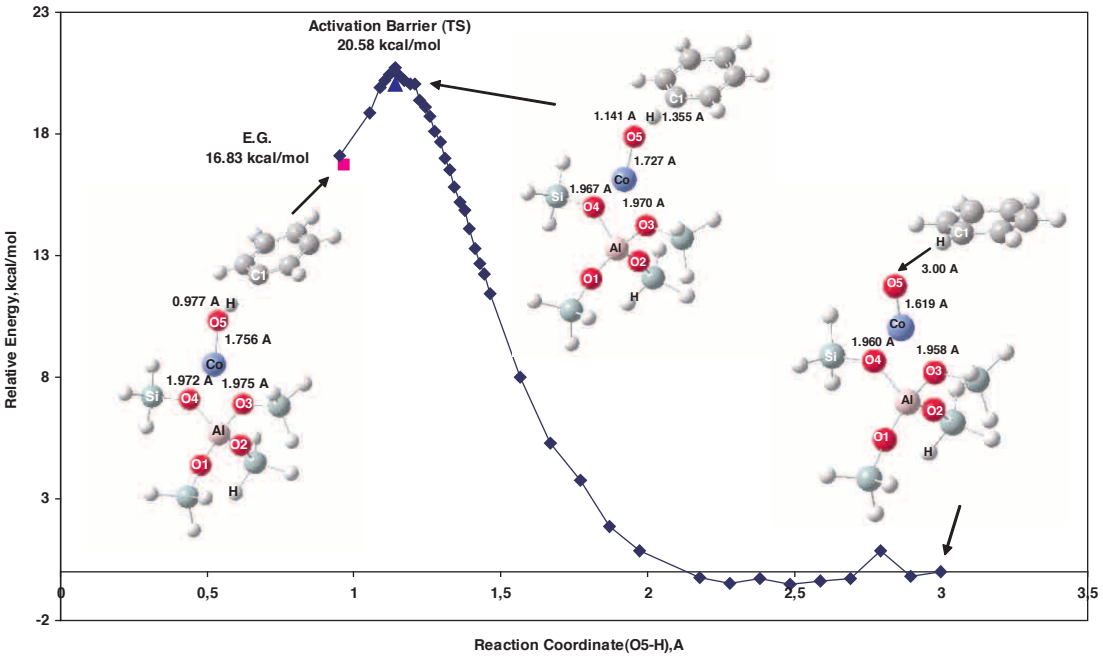

Figure 4. Relative energy profile, transition state, and final equilibrium geometries for C-H bond activation of C_6H_6 (step 2) on CoO-ZSM-5 cluster.

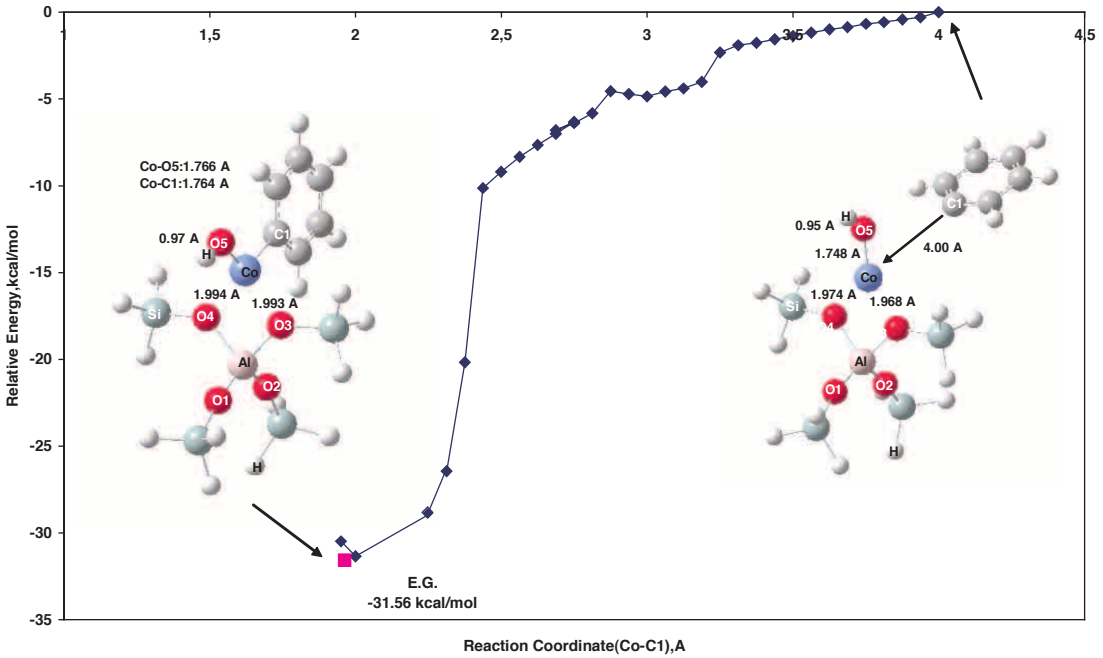

Figure 5. Relative energy profile and final equilibrium geometry for hydroxy complex formation reaction (step 3) on CoO-ZSM-5 cluster.

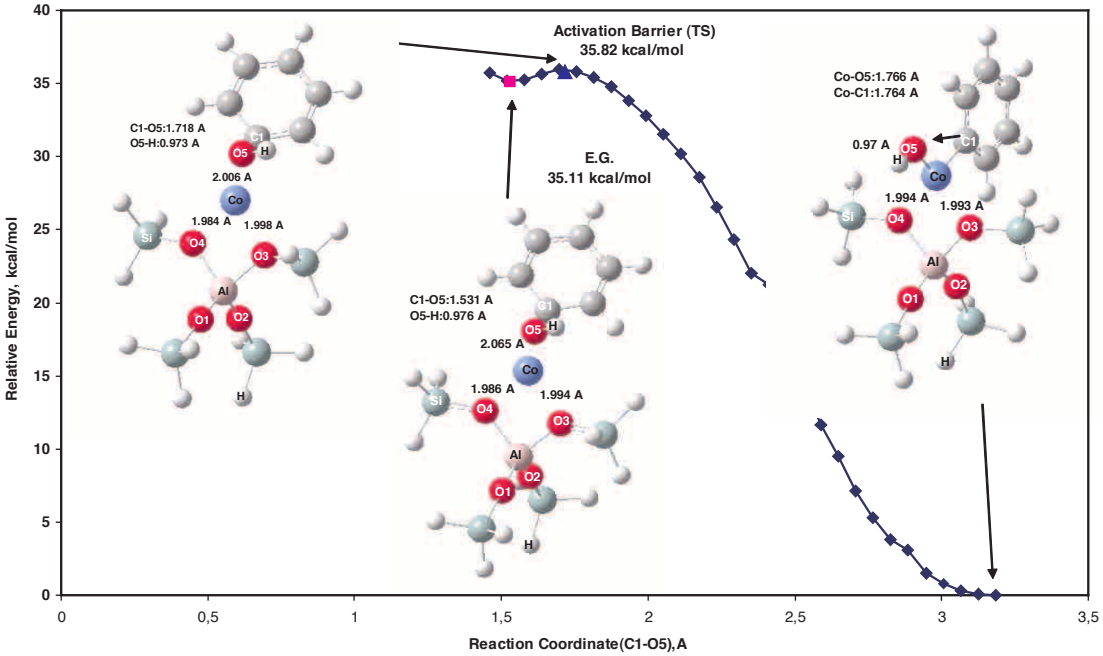

Figure 6. Relative energy profile, transition state and final equilibrium geometries for phenol formation reaction (step 4) on CoO-ZSM-5 cluster.

Finally, the last reaction step (step 5) is desorption of phenol that is formed on the cluster. For this step, a reaction coordinate is selected as the distance between the oxygen atom (O5) of the phenol molecule and Co atom of the cluster. This reaction has a very small desorption barrier of 6.90 kcal/mol as compared to the other steps.

Discussion

A comparison of the activation energy barriers of the direct benzene oxidation to phenol cycle steps on a Fe-ZSM-5 cluster with the available theoretical and experimental literature data is given in the Table. As mentioned before, there are no activation barrier data for the reactions on Co-ZSM-5 in the experimental or theoretical literature. Since surface oxygen is responsible for the formation of phenol from benzene,[2,23,24] the reaction of surface oxygen formation by N_2O on a cluster is a key step in benzene oxidation.

The activation barrier (TS) for step 2 (C-H bond activation of benzene molecule) and step 3 (hydroxy complex formation) was calculated to be 20.29 kcal/mol for the Fe-ZSM-5 cluster. This is close to the theoretical values (17.4 kcal/mol[26] and 23.9 kcal/mol[28]) reported in the literature. Several theoretical studies[26,28] have also reported that hydroxy complex formed on the cluster is stable in energy (-20.80 kcal/mol). The step that has the highest activation barrier is the phenol formation reaction from hydroxy complex formed on the cluster. The activation barrier for this step for Fe-ZSM-5 cluster was calculated to be 45.59 kcal/mol, which is higher than the experimental (30.1 kcal/mol[14]) value reported. There may be several reasons for this discrepancy: **1.** Isolated cations, dimers, and oligonuclear clusters may be present in the Fe- ZSM-5 catalyst as opposed to our

single site model; **2.** our model does not include the effect of the zeolite channel; **3.** experimental conditions such as 648-698 K, feed gas concentration of 30-80 mol% benzene, 1.5-5.0 mol% N_2O, and 0-4.7 mol% phenol as opposed to benzene/N_2O = 1 in this study. Activation barriers for the phenol formation reaction on the Fe-ZSM-5 cluster previously reported in the theoretical literature are given as 31.1 kcal/mol[26], 60.1 kcal/mol[25], and 45.3 kcal/mol[25] on the (FeO_2) center and 51.3 kcal/mol[28] on the (OFeO) center. Yoshizawa et al.[26] have calculated the activation barrier (31.1 kcal/mol) for the phenol formation reaction on a Fe-ZSM-5 cluster by using quartet (4) spin multiplicity. In our study, however, a spin multiplicity number of a sextet (6) was found by SPE calculations for the Fe-ZSM-5 cluster. Ryder et al.[25] have also found and used a spin multiplicity number of a sextet (6) for the oxidation of benzene to phenol over Fe-ZSM-5 cluster modeled as $(SiH_3)_4AlO_4(FeO)$. Since there are some significant differences such as using a smaller cluster and a different spin multiplicity number[26] as well as different active sites[25,28] between the present study and the other theoretical studies, they cannot be directly compared.

Table. Comparison of the activation energy barriers of benzene oxidation to phenol by N_2O on Fe-ZSM-5 cluster and Co-ZSM-5 cluster with literature values.

	Activation Barrier (kcal/mol)			
	Fe-ZSM-5 Cluster		Co-ZSM-5 Cluster	
	This Study	Other Theoretical	This Study	Other Theoretical
Step 1 (N_2O decomposition)	4.41[a]	2.4[b]	6.28[a]	
Step 2 (C-H bond activation of C_6H_6)	20.29	17.4[c] 23.9[e]	20.58	
Step 3 (Hydroxy complex formation)	-	-	0	
Step 4 (Phenol formation)	45.59	31.1[c] 60.1[d] 45.3[d]* 51.3[e]**	35.82	
Step 5 (Phenol desorption)	5.65	20.2[c] 4.5[d] 20.2[d]* 20.1[e]**	6.90	
Global (Experimental)	30.1[f]			

[a] Fellah and Onal[44] (Gaussian/DFT/B3LYP/Cluster)
[b] Yoshizawa et al.[45] (Gaussian/DFT/B3LYP/Cluster)
[c] Yoshizawa et al.[26] (Gaussian/DFT/B3LYP/Cluster)
[d] Ryder et al.[25] (Gaussian/DFT/B3LYP/Cluster)
[e] Yoshizawa et al.[28] (Gaussian/ONIOM/QM:DFT/B3LYP-MM:UFF/Total 2084 Atoms)
[f] Panov et al.[14] (648-698 K, feed gas concentration of 30-80 mol% benzene, 1.5-5.0 mol% N_2O and 0-4.7 mol% phenol)
* Reaction occurs on (FeO_2) center of ZSM-5 Cluster.
** Reaction occurs on (OFeO) center of ZSM-5 Cluster.

The activation barrier for the phenol desorption step is the lowest among all the other steps. In summary, it can be concluded from the present study and from both experimental[14] and theoretical[25,26,28] data that the phenol formation step is the rate-limiting step for benzene oxidation to phenol by N_2O on Fe-ZSM-5.

A similar discussion would be valid for the entire cycle step results for Co-ZSM-5 cluster, which are collected in the Table. In summary, similar activation barrier trends are valid both for Fe-ZSM-5 and Co-ZSM-5 clusters. There are no activation barrier data observed for the reactions on Co-ZSM-5 in the literature. The step that has the highest activation barrier is the phenol formation reaction from hydroxy complex formed on the Co-ZSM-5 cluster. The activation barrier for this step for the Co-ZSM-5 cluster was calculated to be 35.82 kcal/mol, which seems to be lower than the value of 45.59 kcal/mol for the Fe-ZSM-5 cluster. Figure 7 also summarizes the energy diagram of the reaction steps of benzene oxidation cycle for Fe- and Co-ZSM-5 clusters, which for all of the cycle steps' calculated results reported indicate somewhat lower activation barrier values for Co-ZSM-5 in comparison to Fe-ZSM-5 catalysts.

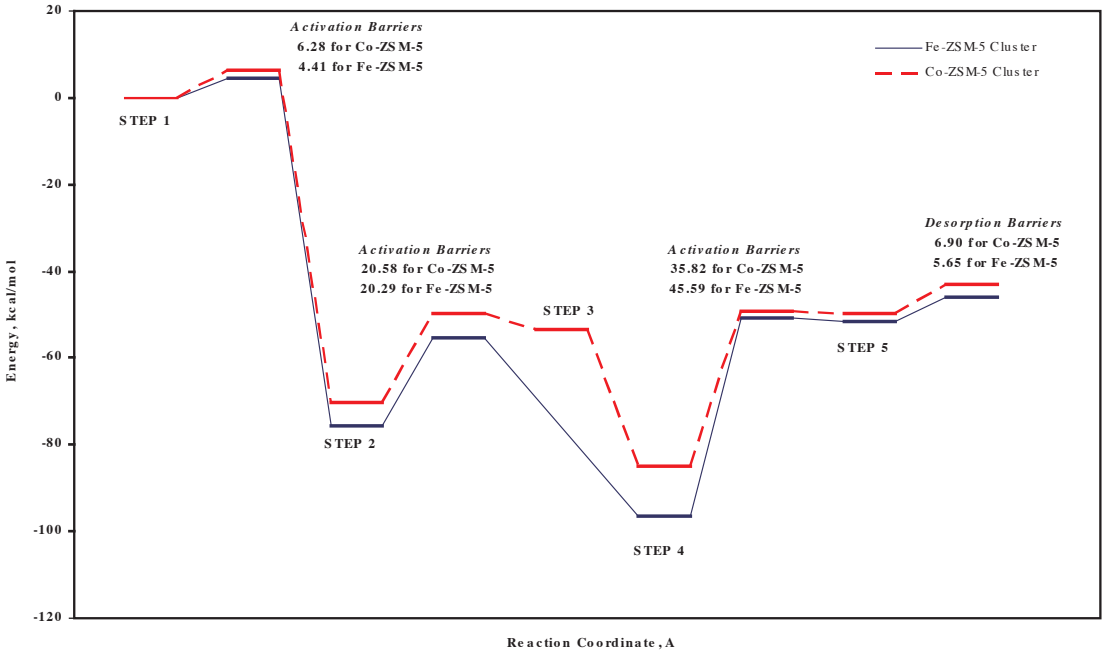

Figure 7. A summary energy diagram showing a comparison of all the steps of benzene oxidation to phenol by N_2O on Fe-ZSM-5 cluster and Co-ZSM-5 cluster.

Conclusions

The steps for the catalytic cycles of benzene oxidation to phenol by N_2O on Fe- and Co-ZSM-5 clusters modeled as $[(SiH_3)_4AlO_4M]$ (M=Fe, Co) are calculated using DFT. The general trend of the results obtained for activation barriers on the Fe-ZSM-5 cluster is in agreement with the experimental and theoretical literature. According to the results obtained, the phenol formation step is the rate-limiting step for both clusters and the Co-ZSM-5 cluster has a lower TS barrier than the TS value obtained for the Fe-ZSM-5 cluster (35.82 kcal/mol

vs. 45.59 kcal/mol). The other type of metal site on ZSM-5 zeolites is the subject of our next study for direct benzene oxidation to phenol.

Acknowledgments

This research was supported in part by TÜBİTAK through TR-Grid e-Infrastructure Project. TR-Grid systems are hosted by TÜBİTAK ULAKBİM and Middle East Technical University. Visit http://www.grid.org.tr for more information.

References

1. Kirk-Othmer, *Encyclopedia of Chemical Technology*, 3rd edition, v.18, p. 747.
2. Panov, G. I. *Cattech* **2000**, *4*, 18-32.
3. Panov, G. I.; Kharitonov, A. S.; Sobolev, V. I. *Appl. Catal. A:Gen.* **1993**, *98*, 1-20.
4. Kharitonov, A. S.; Aleksandrova, T. N.; Panov, G. I.; Sobolev, V. I.; Sheveleva, G. A.; Paukshtis, E. A. *Kinet. Catal.* **1994**, *35*, 270-278.
5. Sobolev, V. I.; Kharitonov, A. S.; Paukshtis, Ye. A.; Panov, G. I. *J. Mol. Catal.* **1993**, *84*, 117-124.
6. Sobolev, V. I.; Dubkov, K. A.; Paukshtis, E. A.; Pirutko, L. V.; Rodkin, M. A.; Kharitonov, A. S.; Panov, G. I. *Appl. Catal. A:Gen.* **1996**, *141*, 185-192.
7. Sheveleva, G. A.; Kharitonov, A. S.; Panov, G. I.; Sobolev, V. I.; Razdobarova, N. L.; Paukshtis, Y. A.; Romannikov, V. N. *Petrol. Chem.* **1993**, *33*, 516-524.
8. Kharitonov, A. S.; Sheveleva, G. A.; Panov, G. I.; Sobolev, V. I.; Paukshtis, Ye. A.; Romannikov, V. N. *Appl. Catal. A:Gen.* **1993**, *98*, 33-43.
9. Sheveleva, G. A.; Panov, G. I.; Kharitonov, A. S.; Romannikov, V. N.; Vostrikova, L. A. *Sibirskii Khemicheskii Zhurnal* **1992**, *3*, 93-96.
10. Panov, G. I.; Sheveleva, G. A.; Kharitonov, A. S.; Romannikov, V. N.; Vostrikova, L. A. *Appl. Catal. A:Gen.* **1992**, *82*, 31-36.
11. Panov, G. I.; Kharitonov, A. S.; Sobolev, V. I. *Appl. Catal. A:Gen.* **1993**, *98*, 1-20.
12. Panov, G. I.; Sheveleva, G. A.; Kharitonov, A. S.; Romannikov, V. N.; Vostrikova, L. *A. Appl. Catal.* **1992**, *82*, 31-36.
13. Volodin, A. M.; Bolshov, V. A.; Panov, G. I. *J. Phys. Chem.* **1994**, *98*, 7548-7550.
14. Ivanov, A. A.; Chernyavsky, V. S.; Gross, M. J.; Kharitonov, A. S.; Uriarte, A. K.; Panov, G. I. *Appl. Catal. A:Gen.* **2003**, *249*, 327-343.
15. Pirutko, L. V.; Chernyavsky, V. S.; Uriarte, A. K.; Panov, G. I. *Appl. Catal. A:Gen.* **2002**, *227*, 143-157.
16. Pillai, K. S.; Jia, J.; Sachtler, W. M. H. *Appl. Catal. A:Gen.* **2004**, *264*, 133-139.
17. Waclaw, A.; Nowinska, K.; Schwieger, W. *Appl. Catal. A:Gen.* **2004**, *270*, 151-156.
18. Yuronov, I.; Bulushev, D.A.; Renken, A.; Kiwi-Minsker, L. *Appl. Catal. A:Gen.* **2007**, *319*, 128-136.

19. Perathoner, S.; Pino, F.; Centi, G.; Giordano, G.; Katovic, A.; Nagy, J. B. *Top. Catal.* **2003**, *23*, 125-136.
20. Hensen, E. J. M.; Zhu, Q.; Janssen, R. A. J.; Magusin, P. C. M. M.; Kooyman, P. J.; van Santen, R. A. *J. Catal.* **2005**, *233*, 123-135.
21. Hensen, E. J. M.; Zhu, Q.; van Santen, R. A. *J. Catal.* **2005**, *233*, 136-146.
22. Chernyavsky, V. S.; Pirutko, L. V.; Uriarte, A. K.; Kharitonov, A. S.; Panov, G. I. *J. Catal.* **2007**, *245*, 466-469.
23. Parmon, V. N.; Panov, G. I.; Uriarte, A.; Noskov, A. S. *Catal. Today* **2005**, *100*, 115-131.
24. Dubkov, K. A.; Sobolev, V. I.; Talsi, E. P.; Rodkin, M. A.; Watkins, N. H.; Shteinman, A. A.; Panov, G. I.; *J. Mol. Catal. A* **1997**, *123*, 155-161.
25. Ryder, J. A.; Chekraborty, A. K.; Bell, A. T. *J. Catal.* **2003**, *220*, 84-91.
26. Yoshizawa, K.; Shiota, Y.; Kagawa, Y.; Yamabe, T. *J. Phys. Chem. B* **2000**, *104*, 734-740.
27. Yoshizawa, K.; Shiota, Y.; Yamabe, *J. Am. Chem. Soc.* **1999**, *121*, 147-153.
28. Shiota, Y.; Suzuki, K.; Yoshizawa, K. *Organometallics* **2006**, *25*, 3118-3123.
29. Kachurovskaya, N. A.; Zhidomirov, G. M.; Hensen, E. J. M.; van Santen, R.A. *Catal. Lett.* **2003**, *86*, 25-31.
30. Kapteijn, F.; Rodreiguez-Mirasol, J.; Moulijn, *J. Appl. Catal. B* **1996**, *9*, 25-64.
31. Kapteijn, F.; Marb, G.; Rodriguez-Mirasol, J.; Moulijn, J. A. *J. Catal.* **1997**, *167*, 256-265.
32. El-Malki, E. M.; van Santen, R. A.; Sachtler, W. M. H.; *J. Catal.* **2000**, *196*, 212-223.
33. Wood, B. R.; Reimer, J. A.; Bell, A. T.; Janicke, M. T.; Ott, K. C. *J. Catal.* **2004**, *224*, 148-155.
34. Zhu, Q.; Mojet, B. L.; Janssen, E. J. M.; van Grondelle, J.; Magusin, P. C. M. M.; van Santen, R. A. *Catal. Lett.* **2002**, *81*, 205-212.
35. Pirngruber, G. D.; Roy, P. K.; Prins, R. *J. Catal.* **2007**, *246*, 147-157.
36. Pirngruber, G. D.; Luechinger, M.; Roy, P. K.; Cecchetto, A.; Smirniotis, P. *J. Catal.* **2004**, *224*, 429-440.
37. Groen, J. C.; Brückner, A.; Berrier, E.; Maldonado, L.; Moulijin, J. A.; Ramirez, J. P. *J. Catal.* **2006**, *243*, 212-216.
38. da Cruz, R. S.; Mascarenhas, A. J. S.; Andrade, H. M. C. *Appl. Catal. B* **1998**, *18*, 223-231.
39. Yakovlev, A. L.; Zhidomirov, G. M.; van Santen, R.A. *Catal. Lett.* **2001**, *75*, 45-48.
40. Yakovlev, A. L.; Zhidomirov, G. M.; van Santen, R.A. *J. Phys. Chem. B* **2001**, *105*, 12297-12302.
41. Heyden, A.; Peters, B.; Bell, A. T.; Keil, F. J. *J. Phys. Chem. B* **2005**, *109*, 1857-1873.
42. Ryder, J. A.; Chakraborty, A. K.; Bell, A. T. *J. Phys. Chem. B* **2002**, *106*, 7059-7064.
43. Yoshizawa, K.; Yumura, T.; Yoshihito, Y.; Yamabe, T.; *Bull. Chem. Soc. Jpn.* **2000**, *73*, 29-36.
44. Fellah, M. F.; Onal, I. *Catal. Today* **2007,** *137*, 410-417
45. Yoshizawa, K.; Yumura, T.; Shiota, Y.; Yamabe, T.; *Bull. Chem. Soc. Jpn.* **2000**, *73*, 29-36.
46. Kohn, W.; Sham, L. *J. Phys. Rev.* **1965**, *140*, A1133-A1138.

47. Gaussian 03, Revision D.01, M. J. Frisch, G. W. Trucks, H. B. Schlegel, G. E. Scuseria, M. A. Robb, J. R. Cheeseman, J. A. Montgomery, Jr., T. Vreven, K. N. Kudin, J. C. Burant, J. M. Millam, S. S. Iyengar, J. Tomasi, V. Barone, B. Mennucci, M. Cossi, G. Scalmani, N. Rega, G. A. Petersson, H. Nakatsuji, M. Hada, M. Ehara, K. Toyota, R. Fukuda, J. Hasegawa, M. Ishida, T. Nakajima, Y. Honda, O. Kitao, H. Nakai, M. Klene, X. Li, J. E. Knox, H. P. Hratchian, J. B. Cross, V. Bakken, C. Adamo, J. Jaramillo, R. Gomperts, R. E. Stratmann, O. Yazyev, A. J. Austin, R. Cammi, C. Pomelli, J. W. Ochterski, P. Y. Ayala, K. Morokuma, G. A. Voth, P. Salvador, J. J. Dannenberg, V. G. Zakrzewski, S. Dapprich, A. D. Daniels, M. C. Strain, O. Farkas, D. K. Malick, A. D. Rabuck, K. Raghavachari, J. B. Foresman, J. V. Ortiz, Q. Cui, A. G. Baboul, S. Clifford, J. Cioslowski, B. B. Stefanov, G. Liu, A. Liashenko, P. Piskorz, I. Komaromi, R. L. Martin, D. J. Fox, T. Keith, M. A. Al-Laham, C. Y. Peng, A. Nanayakkara, M. Challacombe, P. M. W. Gill, B. Johnson, W. Chen, M. W. Wong, C. Gonzalez, and J. A. Pople, Gaussian, Inc., Wallingford CT, 2004.

48. Becke, A. D. *Phys. Rev. B* **1988**, *38*, 3098-3100.

49. Becke, A. D.; Roussel, M. R. *Phys. Rev. A* **1989**, *39*, 3761-3767.

50. Lee, C.; Yang, W.; Parr, R. G. *Phys. Rev. B* **1988**, *37*, 785-789.

51. Lermer, H.; Draeger, M.; Steffen, J; Unger, K. K. *Zeolites* **1985**, *5*, 131-134.

52. Peng, C.; Schlegel, H. B. *Israel J. Chem.* **1993,** *33*, 449-454.

53. Teffo, J. L.; Chedin, A. *J. Mol. Spectroscopy* **1989**, *135*, 389-409.

54. Andzelm, J.; Wimmer, E. *J. Chem. Phys.* **1992**, *96*, 1280-1300.